Proceedings of the Canadian Society for Mechanical Engineering International Congress 2022
CSME Congress 2022
June 5-8, 2022, Edmonton, AB, Canada

Tuning MPC Path-following Controllers Using Multi-objective Optimization

Abbas Ajorkar*, Yuping He
Department of Automotive and Mechatronics Engineering
University of Ontario Institute of Technology, Oshawa, Ontario, L1G 0C5, Canada
*abbas.ajorkar@ontariotechu.net

Abstract— This paper presents a design approach for tuning autonomous driving controllers of road vehicles. In this regard, a bicycle vehicle model and a model predictive control (MPC) algorithm have been applied to the tracking-control lateral of autonomous vehicles. Additionally, in order to maximize ride comfort and minimize path-following error, a multi-objective optimization problem has been formulated. In the multi-objective optimization problem, a meta-heuristic search algorithm, i.e., non-dominated sorting differential evolution (NSDE), is applied, the design objective is to improve ride quality and reduce tracking-control errors, and the design variables are weighting factors of the MPC controller. Numerical simulation is performed to demonstrate the effectiveness of the proposed design approach.

Keywords: autonomous vehicles; tracking-control; path-following; model predictive control; multi-objective optimization; non-dominated sorting differential evolution (NSDE) algorithm

I. INTRODUCTION

Worldwide around 1.35 million people are killed per year in road vehicle accidents [1,2]. Human errors are the main culprits of vast majority of traffic collisions (about 94%) [3]. Hence, in the past two decades, autonomous vehicles (AVs) have been a subject of great attention by researchers. Needless to say, designing an autonomous vehicle platform is a complicated task and contain different tasks, such as sensing, perception, motion-planning, and tracking-control [4]. Tracking-control subsystem is to guide the vehicle autonomously thorough a predefined path.

In the vehicle dynamics community, many studies are focused on the problem of path-following control [5,6]. A proportional-controller was designed to track the predefined path for a road vehicle, and the control gain of the controller was one of the design variables, which were optimized using a genetic algorithm (GA) [7]. In [8], authors designed a robust fractional-order proportional-integral-derivative (FOPID) controller for tracking-control. A particle swarm optimization algorithm was used to optimize the controller parameters. The resulting controller could successfully decrease the tracking error in comparison with conventional PID controllers.

Various control techniques have been applied to the design of trajectory tracking controllers. A robust state feedback lateral controller was introduced for path-following control considering parameter uncertainties and external disturbances [9]. Simulation results showed that this controller outperformed similar controllers in presence of unknown parameters and disturbances. A fuzzy dynamic sliding-mode control was proposed for addressing the path-following problem of AVs [10]. Varied payloads not at the mass center of the AV were tackled, and the comparisons with a fuzzy decentralized path tracking controller confirmed the superiority of the sliding-mode controller.

Among numerous tracking-control techniques, model predictive control (MPC) has gained huge popularity due to its capabilities of systematically handling model uncertainties, as well as state and control constraints, thus, allowing tracking-control to operate at the limits of achievable performance [11]. The essence of MPC is 'prediction', i.e., predicting the future evolution of the system and the future action effects with respect to the model plant [12]. MPC is an optimal control problem, which involves a prediction model [13]. MPC has been extensively used to address the tracking error for multi-input multi-output problems while guaranteeing stability [14].An MPC controller was designed to control longitudinal speed of an AV [15]. The performance of the MPC controller was compared with an PID controller, and the comparison showed that the former decreased the tracking error successfully. An MPC controller was introduced to decrease the lateral deviation and maintain stability at both high and low speeds [16]. Recently, an MPC controller was recommended for maximizing the control performance in tracking speed profile, lateral position, and yaw angle, as well as in improving ride comfort [17]. To this end, a GA was used to tune the weighting factors of the MPC controller offline.

This study proposes an MPC controller for lateral position and yaw angle control for an AV. To maximize the ride comfort and minimize the path-following error, a multi-objective optimization problem is formulated to tune the weighting factors of the MPC controller using a meta-heuristic search algorithm, i.e., non-dominated sorting differential evolution (NSDE).

The rest of the paper is organized as follows. Section II introduces the vehicle kinematic and dynamic model. Section III presents the MPC controller, its objective function and constraints. Section IV defines the multi-objective optimization problem for tuning the weighting matrices of the MPC controller design. Section V introduces the NSDE algorithm for searching the desired solutions to the multi-objective optimization problem. Finally, Section VI presents simulation and results to evaluate the proposed method for improving the MPC controller performance.

II. Vehicle Models

In the motion-planning and tracking-control design for AVs, the predicted paths to be tracked are generally defined in the global coordinate system, while the vehicle dynamic model to be used for tracking-controller design is generated using the vehicle body fixed coordinate system. In this section, the vehicle kinematic and dynamic models are introduced. Note that in the kinematic model, the kinematic data of the AV defined in the body fixed coordinate system are expressed in the global coordinate system.

A. Vehicle Kinematic Model

Figure 1 shows the bicycle vehicle model and the global coordinate system, $X-O-Y$, and the vehicle body fixed coordinate system, $x-o-y$. In the bicycle vehicle model, both the front and rear axle of the vehicle are represented by a single wheel located at the respective axle central point, i.e., A and B. As shown in the figure, δ denotes the steering angle of the front wheel, L the wheelbase, l_r the distance from the center of gravity (CG) of the vehicle to the rear axle, β the vehicle slip angle, θ the vehicle yaw angle measured from X axis, O_1 the instantaneous center of velocity of the vehicle, R the rotating radius of the CG around O_1, and v_f, v, and v_r are the velocity at point A, CG, and B, respectively. Assuming that vehicle forward speed is not very high or R is very large, the following kinematic equation hold,

$$\dot{X} = v\, cos(\theta + \beta) \tag{1}$$

$$\dot{Y} = v\, sin(\theta + \beta) \tag{2}$$

$$\beta = tan^{-1}\left(\frac{l_r\, tan\delta}{L}\right) \tag{3}$$

where $\dot{X}$ and $\dot{Y}$ represent the velocity component at the CG in X and Y axes of the global coordinate system, respectively.

B. Vehicle Dynamic Model

To represent the lateral dynamics of the vehicle and to design the MPC controller for tracking-control of the AV, the governing equations of motion of the bicycle model are derived. To generate the 2 degrees of freedom (DOF) yaw-plane vehicle model, the following assumptions are made: 1) only yaw (θ) and lateral (y) motions are considered; 2) vehicle forward speed remains constant under the specified operating maneuvers; 3) vehicle aerodynamic effect is ignored; and 4) cornering forces of front and rear wheels are related to the corresponding tire slip angle in a linear relationship. Thus, based on Newton's second law, the equations of motion governing the two motions are cast as follows,

$$ma_y = -mv_x\,\dot{\theta} + F_{yf} + F_{yr} \tag{4}$$

$$I_{zz}\ddot{\theta} = l_f F_{yf} - l_r F_{yr} \tag{5}$$

where a_y denotes the lateral acceleration of the vehicle at the CG on y axis, v_x the velocity element on x axis, l_f the distance from the CG to front axle, I_{zz} the yaw mass moment of inertia, F_{yf} and F_{yr} are lateral forces applied to the front and rear tires, respectively. The cornering forces are proportional to the tires slip angle according to the following equations,

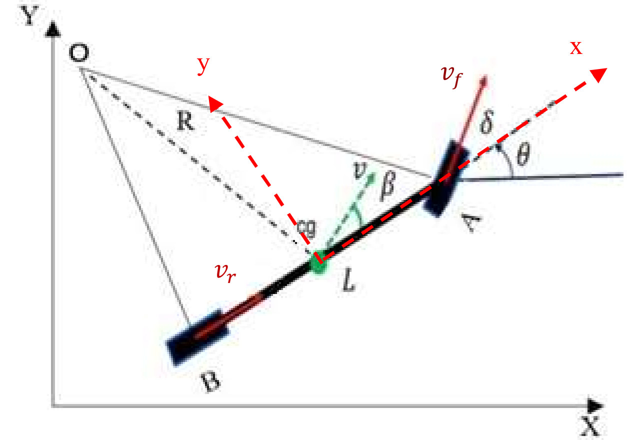

Figure 1. The schematic representation of the bicycle vheicle model [18].

$$F_{yf} = 2C_{\alpha f}\alpha_f = 2C_{\alpha f}\left(\delta - \theta_{Vf}\right) \tag{6}$$

$$F_{yr} = 2C_{\alpha r}\alpha_r = 2C_{\alpha r}(-\theta_{Vr}) \tag{7}$$

where $C_{\alpha f}$ and $C_{\alpha r}$ are the cornering stiffnesses of the front and rear tires, respectively, α_f and α_r the slip angle of the front and rear tires, accordingly. To compute θ_{Vf} and θ_{Vr} in the linear region, the following equations can be used,

$$\theta_{Vf} = \frac{v_y + l_f\dot{\theta}}{v_x} \tag{8}$$

$$\theta_{Vr} = \frac{v_y - l_r\dot{\theta}}{v_x} \tag{9}$$

The vehicle model can be expressed in the state-space form as follows [19],

$$\frac{d}{dt}\begin{bmatrix} y \\ \dot{y} \\ \theta \\ \dot{\theta} \end{bmatrix} = \begin{bmatrix} 0 & 1 & 0 & 0 \\ 0 & -\frac{2C_{\alpha f} + 2C_{\alpha r}}{mv_x} & 0 & -v_x - \frac{2C_{\alpha f}l_f - 2C_{\alpha r}l_r}{mv_x} \\ 0 & 0 & 0 & 1 \\ 0 & -\frac{2C_{\alpha f}l_f - 2C_{\alpha r}l_r}{I_z v_x} & 0 & -\frac{2C_{\alpha f}{l_f}^2 + 2C_{\alpha r}{l_r}^2}{I_z v_x} \end{bmatrix}\begin{bmatrix} y \\ \dot{y} \\ \theta \\ \dot{\theta} \end{bmatrix} + \begin{bmatrix} 0 \\ \frac{2C_{\alpha f}}{m} \\ 0 \\ \frac{2l_f C_{\alpha f}}{I_z} \end{bmatrix}\delta \tag{10}$$

$$\dot{Y} = \dot{y} + \theta v_x \tag{11}$$

where the state and control variable vectors, as well as the output vector are defined as,

$$\boldsymbol{x} = [y \quad \dot{y} \quad \theta \quad \dot{\theta}]^T \tag{12}$$

$$u = \delta \tag{13}$$

$$\boldsymbol{y} = [y \quad \theta]^T \tag{14}$$

III. MPC CONTROLLER

In MPC controller design, a future prediction strategy is introduced to calculate control inputs. In order to ensure the output of the plant (vehicle) follows the reference trajectory (desired path and velocity profile), an MPC controller design is usually formulated as an optimization problem. The optimizer intends to minimize a cost function over the next P time steps (P is prediction horizon) and find the best output solution, which is the nearest one to the reference [20]. However, in each step time, only the first control action is applied.

A. Objective Function

As briefly explained above, an MPC design is essentially an optimization problem over the time window with an objective (cost) function and a set of constraints. The ultimate target of this optimization problem is to minimize the error between the reference output and predicted output over the prediction horizon [21]. In the MPC controller design, the objective function and constraints are defined as follows,

$$J_{mpc} = \sum_{k=0}^{P_H-1} \|\boldsymbol{y}_d(k) - \boldsymbol{y}(k)\|^2{}_{\boldsymbol{Q}} + \sum_{k=0}^{C_H-1} \|\Delta u(k)\|^2{}_R + \sum_{k=0}^{C_H-1} \|u(k)\|^2{}_S \tag{15}$$

$$\begin{gathered} u_{min} \le u(k) \le u_{max} \\ \Delta u_{min} \le \Delta u(k) \le \Delta u_{max} \end{gathered} \tag{16}$$

where P_H and C_H are the prediction horizon and control horizon, respectively, $\boldsymbol{y}_d(k)$ is the reference output vector at the current time step *k,* which is the desired lateral position, $y_d(k)$, and the desired yaw angle, θ_d, $\boldsymbol{y}(k)$ denotes the predicted output vector, including the lateral position, $y(k)$, and the yaw angle, $\theta(k)$, and $u(k)$ is the current input of the plant, which is the steering angle of the vehicle, δ, and $\boldsymbol{Q}$, R, and S are the respective weighting matrix and factors. The selection of the weighting matrix and factors, $\boldsymbol{Q}$, R, and S, reflects our control objective to keep the tracking error, $\|\boldsymbol{y}_d(k) - \boldsymbol{y}(k)\|$, 'small' using the control actions, $\|\Delta u(k)\|$ and $\|u(k)\|$, that are 'not too large'.

B. Reference Trajectory

In this study, the reference trajectory is considered as the predefined path for a single lane-change maneuver at a constant forward speed. As shown in Figure 2, the predefined path is defined in the global coordinate system, X-O-Y.

IV. MULTI-OBJECTIVE OPTIMIZATION

To tune the weighting matrix, $\boldsymbol{Q}$, and weighting factors R, and S for the MPC controller, a multi-objective optimization problem is formulated as shown in Figure 3. Essentially, this is a bi-layer optimization problem [22,23]. At the upper layer, the weighting the weighting matrix, $\boldsymbol{Q}$, and weighting factors R, and S for the MPC controller are treated as design variables, and a meta-heuristic algorithm, i.e., NSDE, is selected as the search algorithm for the multi-objective optimization problem. The objective function of the multi-objective optimization and constraints are defined as,

$$\min_{\boldsymbol{Q},R,S} J(\boldsymbol{Q}, R, S) = w_1 J_1 + w_2 J_2 \tag{17}$$

subject to:

$$q_{li} \le Q_i \le q_{ui},\ i = 1, 2 \tag{18}$$

$$r_l \le R \le r_u \tag{19}$$

$$s_l \le S \le s_u \tag{20}$$

where J_1 and J_2 are the vehicle dynamic responses associated with the ride comfort and path-following error over the single lane-change maneuver, w_1 and w_2 the respective weighting factors, Q_i denotes the diagonal element of $\boldsymbol{Q}$, q_{li} and q_{ui} are the lower and upper bounds, r_l and r_u the lower and upper bounds of the weighting factor R, and s_l and s_u the lower and upper bounds of the weighting factor *S*.

With a given set of design variables in terms of $\boldsymbol{Q}$, R and S provided from the upper layer, an effective search algorithm, e.g., sequential quadratic programming (SQP), may be used to solve the MPC optimization problem to find optimal control inputs for the AV. Then, the corresponding fitness value of the MPC optimization problem, J_{mpc}, will be returned to the upper level. At this point, if the specified criteria are satisfied, the optimization will be terminated, and the optimal solutions in terms of $\boldsymbol{Q}$, R and S are identified. Otherwise, the NSDE algorithm will conduct another round of search of the design variables in the design space, and the previous process will repeat until the optimal solutions are found.

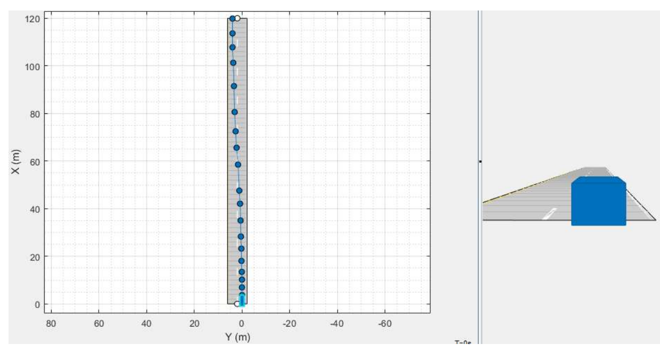

Figure 2. The predefinded reference path for the single lane-change maneuver.

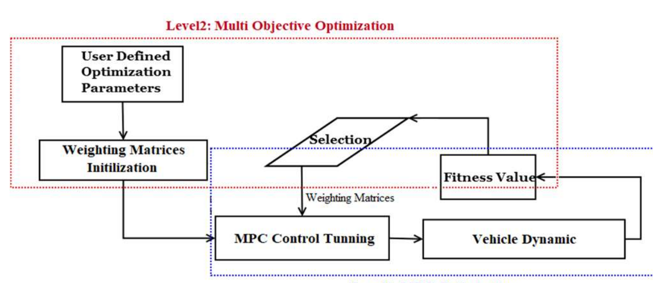

Figure 3. The bi-layer optimization scheme for tuning the weighting factors for the MPC controller.

In the following subsections, we define the vehicle dynamic responses associated with the ride comfort (J_1) and path-following error (J_2) over the single lane-change maneuver.

A. Ride Comfort

As introduced in Section II, this study only considers the lateral dynamics of the AV. To evaluate the ride comfort of the AV over the specified single lane-change maneuver, the root of mean square (RMS) value of the lateral acceleration (a_Y) can be used as an effective performance indicator [17]. Assuming that the time duration of the single lane-change maneuver is T_T, the ride comfort performance measure is determined by

$$J_1 = a_{eq} = (a_Y)_{RMS} = \sqrt{\frac{1}{T_T}\int_{t=0}^{t=T_T} a_Y(t)^2 dt} \quad (21)$$

B. Path-Following Error

To evaluate the path-following performance of the MPC controller, we select the integral of the square error (ISE) between the vehicle output and their references as the indicator [24]. The ISE index is defined by

$$J_2 = ISE = \int_{t=0}^{t=T_T} e(t)^2 dt \quad (22)$$

where e(t) is the signal error between the vehicle output and their references.

V. NSDE ALGORITHM

In this section, the NSDE algorithm used to the upper layer optimization shown in Figure 3 is introduced.

NSDE algorithm is a simple extension of differential evolution (DE) technique for finding pareto optimal solution to multi-objective optimization problems. It consists of two main parts: 1) a DE optimization algorithm for the mutation and crossover; and 2) an elitist non-dominated sorting algorithm for selection.

A. Differential Evolution

DE is a population-based metaheuristic optimization algorithm, which was introduced in 1997 [25]. DE optimizes a problem by maintaining a population of candidate solutions and creating new candidate solutions by combining existing ones according to its simple formulae, and then keeping whichever candidate solution has the best score or fitness on the optimization.

B. Elitist Non-Dominated Sorting

In the part of selection of NSDE, an elitist non-nominated sorting algorithm has been employed to find the pareto optimal front. The algorithm includes two main parts [26].

1) Fast nondominated sorting

The algorithm identifies and divides all solutions in different nondominated front level in the objective function space.

2) Diversity preservation

Along with the convergence to optimal pareto front set, it is very important that the algorithm maintains a good spread of solutions in the obtained set of solutions. In this part, acceptance or rejection of a solution is based on the density estimation which is measured by crowding distance criterion.

VI. SIMULATION RESULTS

To examine the proposed design method and the MPC controller, a virtual single lane-change maneuver is implemented using numerical simulation. Figure 4 shows the specified path for this single lane-change maneuver. Table I lists the parameters for the 2-DOF vehicle model and those for designing the MPC controller.

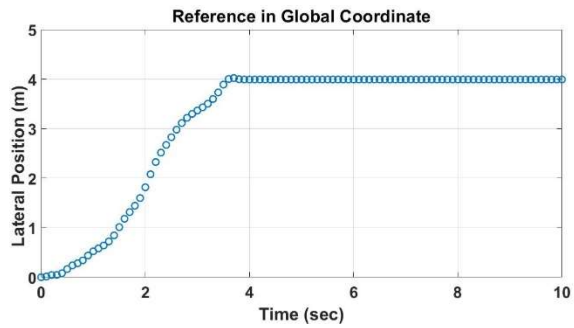

Figure 4. The predefined path for the single lane-change maneuver.

TABLE I. PARAMETERS FOR THE 2-DOF VEHICLE MODEL AND MPC CONTROLER DESIGN

Vehicle Parameters						
m (Kg)	v_x (m/sec)	I_z $(Kg.m^2)$	l_f (m)	l_r (m)	C_f (N/rad)	C_f (N/rad)
1730	15	3000	2	2	80000	80000
MPC Controller Parameters						
u_{min}	u_{max}	Δu_{min}	Δu_{max}	P_H	C_H	$\Delta t(sec)$
$-\pi/6$	$\pi/6$	$-\pi/12$	$\pi/12$	10	2	0.1

Figure 5 shows the optimal pareto front for the two design criteria, i.e., J_1 indicating the ride comfort (a_{eq}), and J_2 indicating cumulative path-following error between reference signals and outputs over the single lane-change maneuver.

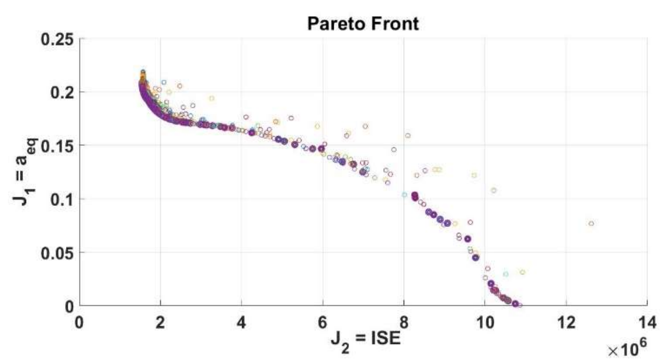

Figure 5. The optimal pareto front of the two design criteria over the single lane-chagne maneuver.

Table II shows the evaluation levels of human ride comfort based on the equivalent RMS acceleration specified by ISO 2631-1 [17].

Figure 5 indicates that the RMS acceleration value of the AV does not exceed from $0.23\ m/s^2$ under the maneuver, which is less than $0.315\ m/s^2$ specified in Table II. Hence, over the single lane-change maneuver, the driver and passengers are always in the comfort zone for all points on the pareto front. Therefore, the design criterion of J_2 is to be emphasized for the multi-objective optimization problem, and the design variables, i.e., the weighting matrix and factors, $\boldsymbol{Q}$, R, and S, are optimized with the consideration of minimizing the performance index J_2. Figure 6 shows the fitness value of J_2 versus the generation number of the NSDE algorithm.

TABLE II. EVALUATION LEVELS OF HUMAN RIDE COMFORT BY ISO-2631-1 [17]

$a_{eq} \leq 0.315\, m/s^2$	Not uncomfortable
$0.315\, m/s^2 \leq a_{eq} \leq 0.63\, m/s^2$	A little uncomfortable
$0.5\, m/s^2 \leq a_{eq} \leq 1.0\, m/s^2$	Fairly uncomfortable
$0.8\, m/s^2 \leq a_{eq} \leq 1.6\, m/s^2$	Uncomfortable
$1.25\, m/s^2 \leq a_{eq} \leq 2.5\, m/s^2$	Very uncomfortable
$a_{eq} \geq 2.0\, m/s^2$	Extremely uncomfortable

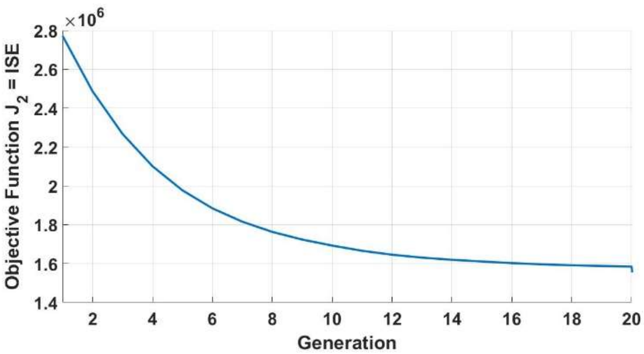

Figure 6. The fitness value of J_2 versus the generation number of the NSDE algorithm.

The optimal weighting matrix and factors for minimizing the performance index, J_2, are shown as follows,

$$\boldsymbol{Q} = \begin{bmatrix} 34.5 & 0 \\ 0 & 53.68 \end{bmatrix}, R = [24.20], S = [66.15] \qquad (23)$$

To examine the performance of the finely tuned MPC controller, simulations have been conducted considering two cases: 1) the baseline design of the MPC controller without tuning the weighting matrix and factors; and 2) the optimal design of the MPC controller with the weighting matrix and factors taking the values shown in (21). For the baseline design, the path-following result and the lateral position error between the reference signal and vehicle lateral displacement are shown in Figure 7 and 8, respectively.

Figures 7 and 8 show that the baseline design can follow the reference path and completes the lane-change successfully, but the maximum vehicle lateral position error is not satisfactory. As shown in Figure 8, at t = 2.3 s, the vehicle lateral position error is approximately 1 m, which is large for an AV tracking-control under the single lane-change maneuver.

For the optimal design, Figures 9 and 10 illustrate the path-following result and the vehicle lateral position error between the reference signal and vehicle lateral displacement, respectively.

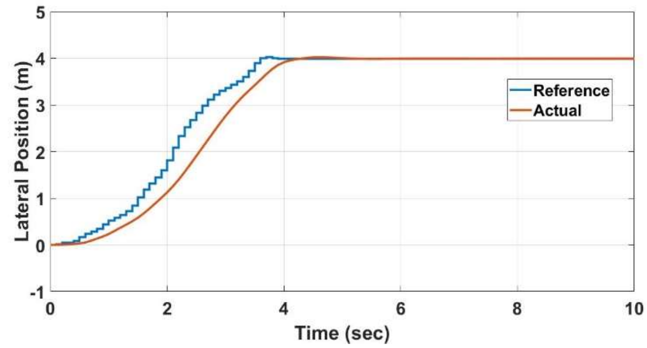

Figure 7. Time history of the reference and actual vehicle lateral position for the baseline design.

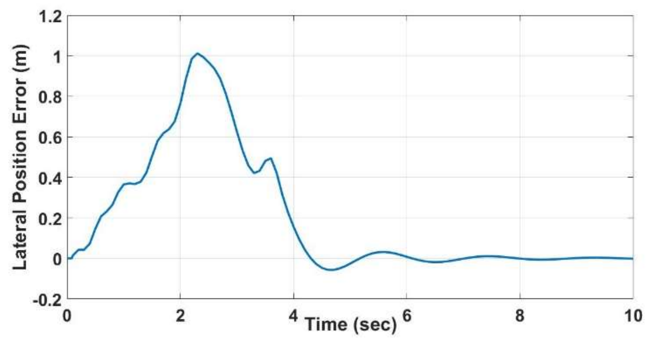

Figure 8. Time history of the vehicle lateral position error for the baseline design.

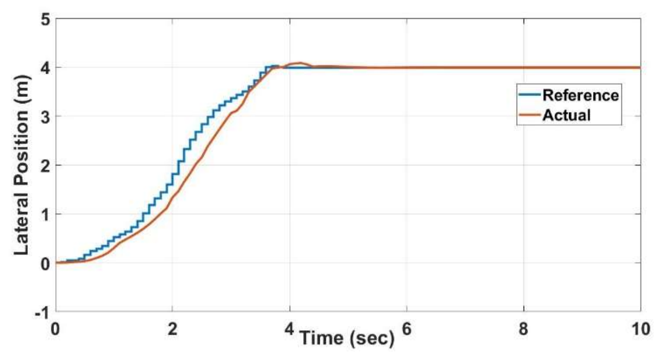

Figure 9. Time history of the reference and actual vehicle lateral position for the optimal design.

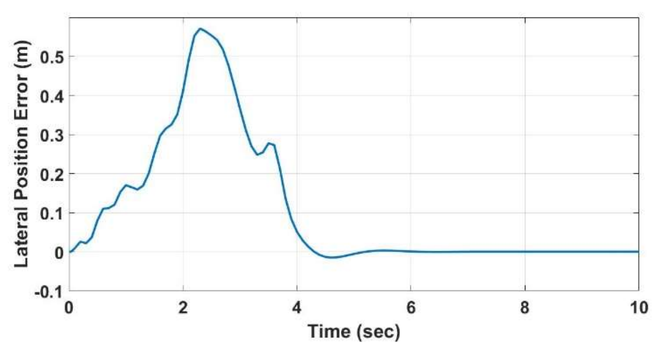

Figure 10. Time history of the vehicle lateral position error for the optimal design.

As shown in Figures 9 and 10, the optimal design can track the reference path and successfully execute the lane-change maneuver with improved performance in comparison with the baseline design. The lateral error is decreased considerably. As shown in Figure 10, at t = 2.3 sec, the optimal design decreases the vehicle lateral position error by 42% (from 1 m to 58 cm) compared against the baseline design. It must be mentioned that for the optimal MPC controller with weighing matrix and factors tuned, the performance indices J_1 and J_2 take the fitness values of 0.23 and 1.66×10^6, respectively.

VII. Conclusions

This paper presented a novel tuning method for designing an MPC controller for autonomous vehicle tracking-control. Based on the multi-objective metaheuristic optimization approach, the weighing matrices in the MPC controller design has been tuned to minimize the path-following error and the RMS value of vehicle lateral acceleration. To evaluate the effectiveness of the proposed approach, a single lane-change maneuver has been simulated. Simulation results demonstrate that the proposed algorithm can successfully tune weighting matrices for the MPC controller for improving path-following performance and enhancing ride comfort.

References

[1] World Health Organization, "Global Status Report on Road Safety 2018". [cited 2021 Dec.5]. Available from: https://www.who.int/publications/i/item/9789241565684

[2] Z. Ni and Y. He, "Design and validation of a robust active trailer steering system for multi-trailer articulated heavy vehicles," Vehicle System Dynamic, vol. 57, no.10, pp.1545-1571, 2019.

[3] Standing Senate Committee on Transport and Communications, "Driving Change: Technology and the Future of the Automated Vehicle", Report of the Standing Senate Committee on Transport and Communications. 2018; Senate, Ottawa, Ontario, Canada. Available from: https://sencanada.ca/content/sen/committee/421/TRCM/Reports/COM_RPT_TRCM_AutomatedVehicles_e.pdf

[4] A. Rahimi and Y. He, "A Review of Essential Technologies for Autonomous and Semi-autonomous Articulated Heavy Vehicles," Proceedings of the Canadian Society for Mechanical Engineering International Congress 2020, June 21-24, 2020, Charlottetown, PE, Canada.

[5] S. Zhu and Y. He, "A unified lateral preview driver model for road vehicles," IEEE Transactions on Intelligent Transportation Systems, vol. 21, no.11, pp. 4858–4868, 2020.

[6] M.M. Islam, X. Ding, and Y. He, "A closed-loop dynamic simulation-based design method for articulated heavy vehicles with active trailer steering systems," Vehicle System Dynamics, vol. 50, no.5, pp. 675–697, 2012.

[7] Y. He, M.M. Islam, S. Zhu, and T. Hu, "A design synthesis framework for directional performance optimization of multi-trailer articulated heavy vehicles with trailer lateral dynamic control systems," Proc IMechE Part D: J Automobile Engineering, vol. 231, no. 8, pp. 1096–1125, 2017.

[8] A. Al-Mayyahi, W. Wang, and P. Birch, "Design of fractional-order controller for trajectory tracking control of a non-holonomic autonomous ground vehicle," Journal of Control, Automation and Electrical Systems, vol. *27*, no.1, pp. 29–42, 2016.

[9] R. Wang, H. Jing, C. Hu, F. Yan, and N. Chen, "Robust H_∞ path following control for autonomous ground vehicles with delay and data dropout," IEEE Transactions on Intelligent Transportation Systems, vol.17, no.7, pp. 2042–2050, 2016.

[10] C.-L. Hwang, C.-C. Yang, and J.Y. Hung, "Path tracking of an autonomous ground vehicle with different payloads by hierarchical improved fuzzy dynamic sliding-mode control," IEEE Transactions on Fuzzy Systems, vol.26, no.2, pp. 899–914, 2018.

[11] P. Falcone, H. E. Tseng, F. Borrelli, et al., "MPC-based yaw and lateral stabilisation via active front steering and braking," Vehicle System Dynamics, vol 46, supplement, pp. 611-628, 2008.

[12] A. Rahimi, W. Huang, T. Sharma, and Y. He, "An autonomous driving control strategy for multi-trailer articulated heavy vehicle with enhanced active trailer safety," the 27th IAVSD Symposium on Dynamics of Vehicles on Roads and Tracks, Saint-Petersburg, Russia, p.12, August 16-20, 2021.

[13] L. Liu, B. Wang, and Y. He, "Research on path-tracking control of articulated vehicle with a trailer based on advanced model prediction control strategy," Proceedings of the Canadian Society for Mechanical Engineering International Congress 2021, June 27-30, 2021, Charlottetown, PE, Canada.

[14] F. Yakub, A. Abu, S. Sarip, and Y. Mori, "Study of model predictive control for path-following autonomous ground vehicle control under crosswind effect," Journal of Control Science and Engineering, vol. 2016, pp.1–18, 2016.

[15] L. Pacheco and N. Luo, "Testing PID and MPC performance for mobile robot local path-following," International Journal of Advanced Robotic Systems, vol. 12, p.13, 2016.

[16] C. Sun, X. Zhang, Q. Zhou, and Y.Tian, "A model predictive controller with switched tracking error for autonomous vehicle path tracking," IEEE Access, vol. 7, pp. 53103–53114, 2019.

[17] S. Luciani, A. Bonfitto, N. Amati, and A.Tonoli, "Model predictive control for comfort optimization in assisted and driverless vehicles," Advances in Mechanical Engineering, vol.12, no. 11, pp.1-14, 2020.

[18] J. Dallas, J. Wurts, J.L. Stein, and T. Ersal, "Contingent nonlinear model predictive control for collision imminent steering in uncertain environment," IFAC PapersOnLine, vol.53, no.2, p.14330-14335, 2020.

[19] R. Rajamani, R. Vehicle dynamics and control, 2nd ed., Mechanical Engineering Series, New York, Heidelberg: Springer, 2012.

[20] Y. Mizushima, I. Okawa, and K. Nonaka, "Model predictive control for autonomous vehicles with speed profile shaping," IFAC Papers On Line, vol. 52, no.8, pp.31–36, 2019.

[21] J. Yu, T, Sharma, and Y. He, "Design optimization of autonomous steering control schemes for articulated vehicles," Progress of the Canadian Society for Mechanical Engineering International Congress, June 27-30, 2021, Charlottetown, PE, Canada.

[22] Y. He and M.M. Islam, "An automated design method for active trailer steering systems for articulated heavy vehicles," Journal of Mechanical Design, vol. 134, no. 4, p.15, 2012.

[23] Y. He and J. McPhee, "Multidisciplinary design optimization of mechatronic vehicles with active suspensions," Journal of Sound and Vibration, vol. 283, pp.217-241, 2005.

[24] A. Rodríguez-Molina, E. Mezura-Montes, M.G. Villarreal-Cervantes, and M. Aldape-Pérez, "Multi-objective meta-heuristic optimization in intelligent control: A survey on the controller tuning problem," Applied Soft Computing, vol. 93, 106342, 2020.

[25] R.M. Storn and K. Price, "Differential evolution – a simple and efficient heuristic for global optimization over continuous spaces," Journal of Global Optimization, vol. 11, pp. 341–359, 1997.

[26] K. Deb, A. Pratap, S. Agarwal, and T. Meyarivan, "A fast and elitist multi objective genetic algorithm: NSGA-II," IEEE Transactions on Evolutionary Computation, vol. 6, no. 2, pp.182–197, 2002